Mean vertical motion and non-adiabatic heat sources over India during the monsoon

By P. K. DAS, *Meteorological Office, New Delh, India*

(Manuscript received June 27, 1961)

ABSTRACT

The mean vertical velocity in pressure coordinates, and the corresponding height tendency, was computed at intervals of 100 mb from 1000 mb to 50 mb on a mesh covering India and most of southeast Asia. The rate of non-adiabatic heat supply was expressed as a function of the computed height tendency. The results showed pronounced ascent over northeast India and a zone of subsidence over northwest India. The rate of ascent decreased uniformly with pressure suggesting force ascent on account of orographic features to the north of India. The computed values of the height tendency indicated that non-adiabatic heat sources must be capable of producing an average warming at the rate of 1.6 C(12hr)$^{-1}$ in northeast India, and an average cooling by 1.2 C(12hr)$^{-1}$ in northwest India.

1. Introduction

The present paper is an attempt to study the variation of mean vertical motion with pressure, and to examine its relation with non-adiabatic heat sources. In view of its synoptic interest, we chose mean isobaric contours for a typical monsoon month (July), and the area selected for study covered India and most of the adjoining regions of southeast Asia. The mean vertical velocity was computed in pressure coordinates with the help of a geostrophic ten-layer model.

In dealing with mean motion it is customary to neglect time derivatives in the relevant equations, but a different procedure was adopted in this paper. We derived an equation for ϕ_t, the height tendency of a constant pressure surface, by eliminating vertical velocity from equations representing the conservation of vorticity and entropy. The forcing function of this equation contained a term for the rate of non-adiabatic heat supply. The requirements of a steady state ($\phi_t = 0$) were then satisfied by making the forcing function, and the inhomogeneous part of the lower boundary condition, vanish. In this manner, we obtained the non-adiabatic heating which would make the motion steady. The advantage of this procedure was that it enabled us to estimate the non-adiabatic heat supply in terms of the variation of ϕ_t with pressure.

2. Geostrophically defined heating (Q)

Under the usual approximations based on scale considerations (CHARNEY, 1948), we may express the conservation of vorticity and entropy in the familiar form

$$\nabla^2\phi_t + f\mathbf{V}\cdot\nabla\eta = f^2\frac{\partial\omega}{\partial p} \tag{2.1}$$

$$\phi_{pt} + \mathbf{V}\cdot\nabla\phi_p = -\sigma\omega - \frac{kQ}{p}, \tag{2.2}$$

where Q represents the rate of non-adiabatic heating (kj ton^{-1} sec^{-1}), $k = R/c_p$, η stands for the absolute vorticity, σ the stability parameter

$$\left(-\frac{1}{\varrho}\frac{\partial}{\partial p}\ln\theta\right),$$

f is the Coriolis parameter, ϕ represents geopotential and ω is the vertical pressure-velocity. We have used subscripts to denote derivatives, and friction has been neglected in (2.1).

Eliminating ω we have

$$L(\phi_t) = -f\mathbf{V}\cdot\nabla\eta - \frac{\partial}{\partial p}\left(\frac{f^2}{\sigma}\mathbf{V}\cdot\nabla\phi_p\right) - \frac{\partial}{\partial p}\left(\frac{Kf^2Q}{\sigma p}\right), \tag{2.3}$$

where $$L \equiv \left[\nabla^2 + \frac{\partial}{\partial p}\left(\frac{f^2}{\sigma}\frac{\partial}{\partial p}\right)\right]. \quad (2.4)$$

The boundary conditions are

$$(\omega)_1 = 0, \quad (2.5)$$

$$(\phi_t)_0 = (gw)_0 - \frac{1}{(\sigma\varrho)_0}\left[\frac{kQ}{p} + (\mathbf{V}\cdot\nabla\phi_p)_0\right]. \quad (2.6)$$

Subscripts 1 and 0 refer to conditions at the top of the atmosphere and the lower boundary ($p_0 = 1000$ mb). w_0 is the vertical velocity at the top of the friction layer and is determined by orographic uplift and frictional convergence.

We are interested in the mean vertical motion corresponding to a steady state. Consequently, ϕ_t must vanish throughout the range of integration of (2.3). This will be the case if the inhomogeneous parts of (2.3) and (2.6) vanish. On imposing this constraint we have

$$\frac{KQ_0}{p_0} = -(\mathbf{V}\cdot\nabla\phi_p)_0 + g(\sigma\varrho w)_0, \quad (2.7)$$

$$\frac{\partial}{\partial p}\left(\frac{fQK}{\sigma p}\right) + \mathbf{V}\cdot\nabla\eta + \frac{\partial}{\partial p}\left(\frac{f}{\sigma}\mathbf{V}\cdot\nabla\phi_p\right) = 0. \quad (2.8)$$

Integrating (2.8) between the limits p and p_0, and using (2.7) for Q_0, we are led to the following expression for Q

$$\frac{KQ}{p} = -\mathbf{V}\cdot\nabla\phi_p + \sigma(g\varrho w)_0 - \sigma\int_{p_0}^{p}\frac{\mathbf{V}\cdot\nabla\eta}{f}dp. \quad (2.9)$$

This field of heating is such that ϕ_t determined from (2.3), (2.5) and (2.6) will vanish.

Equation (2.9) was not used directly. Instead, a field of ϕ_t was first computed from (2.3) and (2.6) under the assumption that $Q = 0$. Using the symbol ϕ_t^* for this new field, we may define ϕ_t^* as the solution of the adiabatic versions of (2.3) and the boundary conditions (2.5) and (2.6). Thus

$$L(\phi_t^*) = -f\mathbf{V}\cdot\nabla\eta - \frac{\partial}{\partial p}\left(\frac{f^2}{\sigma}\mathbf{V}\cdot\nabla\phi_p\right), \quad (2.10)$$

and $$(\phi_t^*)_0 = gw_0 - \frac{1}{\varrho_0\sigma_0}(\varphi_{pt}^* + \mathbf{V}\cdot\nabla\phi_p)_0. \quad (2.11)$$

A corresponding field of ω^* will be also defined by (2.1), which will be the adiabatic version of (2.2) with ϕ_t replaced by ϕ_t^*.

We may now express the advective term $(\mathbf{V}\cdot\nabla\eta)$ in (2.9) in terms of the adiabatically computed ϕ_t^* defined by (2.10) and (2.11). We have

$$\sigma\int_{p_0}^{p}\frac{\mathbf{V}\cdot\nabla\eta}{f}dp = -\frac{\sigma}{f^2}\int_{p_0}^{p}\nabla^2\phi_t^*dp + \frac{\sigma}{\sigma_0}(\phi_{pt}^* + \mathbf{V}\cdot\nabla\phi_p)_0 - (\phi_{pt}^* + \mathbf{V}\cdot\nabla\phi_p),$$

whence

$$\frac{KQ}{p} = \phi_{pt}^* - \sigma\omega_0^* + \frac{\sigma}{f^2}\int_{p_0}^{p}\nabla^2\phi_t^*\,dp. \quad (2.12)$$

3. Computational procedure

Equation (2.10) was solved by three dimensional relaxation at each grid point. The procedure was similar to that outlined by CHARNEY and PHILLIPS (1953), except that the more exact relation (2.11) was used as the lower boundary condition. The effects of ground friction and irregularities of the surface terrain were partially incorporated in the expression for the surface vertical velocity (w_0). Thus

$$w_0 = L\zeta_0 + (\mathbf{V}\cdot\nabla H)_0, \quad (3.1)$$

where $L = 200$ m and H stands for contours of the ground. Space averaged values of H prepared by BERKOFSKY and BERTONI (1955) were used in this investigation.

The relaxation was carried out on a 24×26 grid for the horizontal coordinates. Ten pressure levels from 95 cb to 5 cb, with intervals of 10 cb, formed the vertical grid. The programme for machine computation evaluated the height tendency (ϕ_t^*) for the levels 5, 15, ... 95 cb, while ω^* was defined for 0, 10, ... 100 cb.

For the present investigation a Lambert conformal map of southeast Asia was constructed with standard parallels at 10 N and 40 N. This minimizes the variations of the map scale factor. Computation of the scale factor at different sectors of the map revealed a maximum distortion of the order of only six per cent between the centre and the edges of the map. The variation of the scale factor was therefore

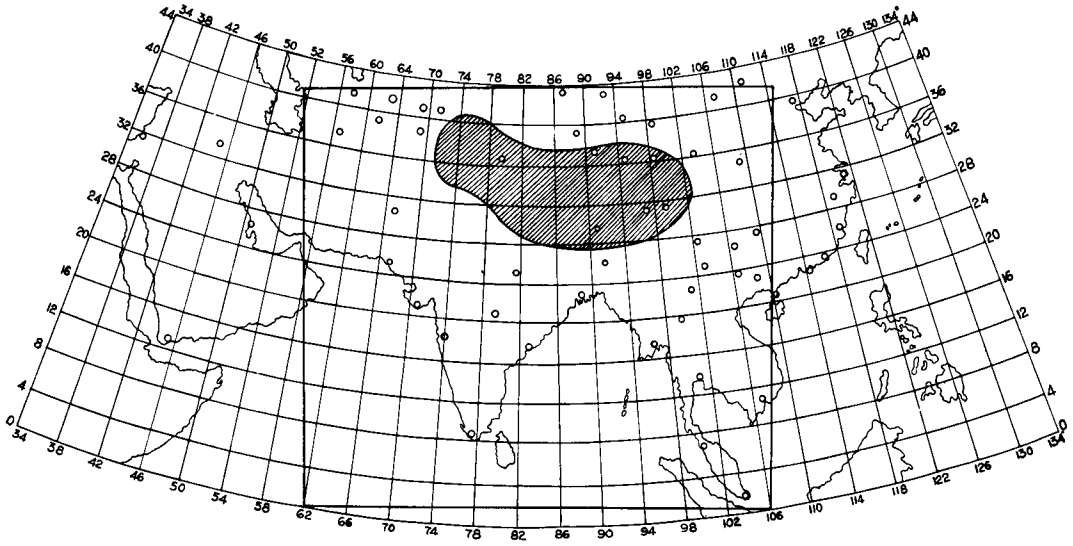

FIG. 1. Location of finite-difference lattice. Large rectangle outlines grid used for computation; area under hatching indicates terrain 10,000 feet above mean sea level. Circles represent network of upper air stations.

neglected in the computation. A grid increment of approximately 200 km was used. The size of the grid is shown in Fig. 1.

In Figs. 2, 3 and 4 we present the mean isobaric pattern for 850, 500 and 100 mb over southeast Asia for the month of July. These maps were prepared from all available climatological means of upper air data from India and the neighbouring countries of southeast Asia. Monthly means for July were also prepared for fifty stations in the U.S.S.R. and the Chinese mainland on the basis of two years daily records (1957 and 1958) of data published by the U.S. Weather Bureau. In addition to the above charts, isobaric charts were also constructed for 1000, 700, 400, 300, 100 and 50 mb. To save

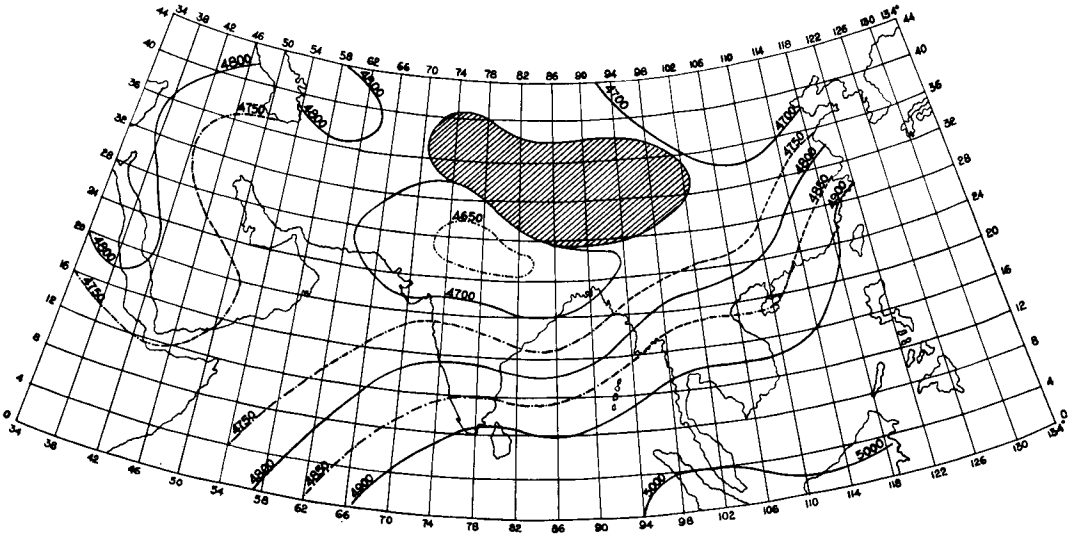

FIG. 2. Mean isobaric contours in feet for July: 850 mb.

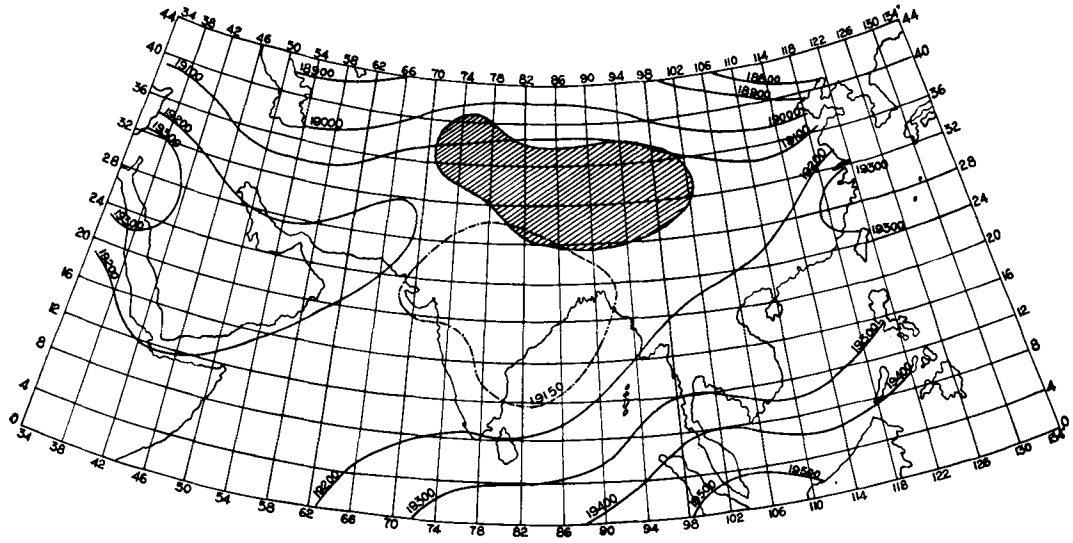

FIG. 3. Mean isobaric contours in feet for July: 500 mb.

space they are not reproduced here, but all the charts were used in the computation.

Two main features of the monsoon circulation are brought out in Figs. 2, 3 and 4. Firstly, we notice a decrease in the intensity of the monsoon from the surface to about 500 mb, and a reversal above 500 mb. The flow pattern in the upper troposphere is governed by a quasi-static anticyclone with a well-marked westerly jet along its northern edge. The southern periphery of this anticyclone is also marked by strong winds which are sometimes referred to as the eastern jet. The second feature of importance is the absence of any pronounced flow perpendicular to the mountain ranges. An examination of the upper wind data from several stations on the southwestern boundary of the mountains indicated a cross mountain flow (downslope) of

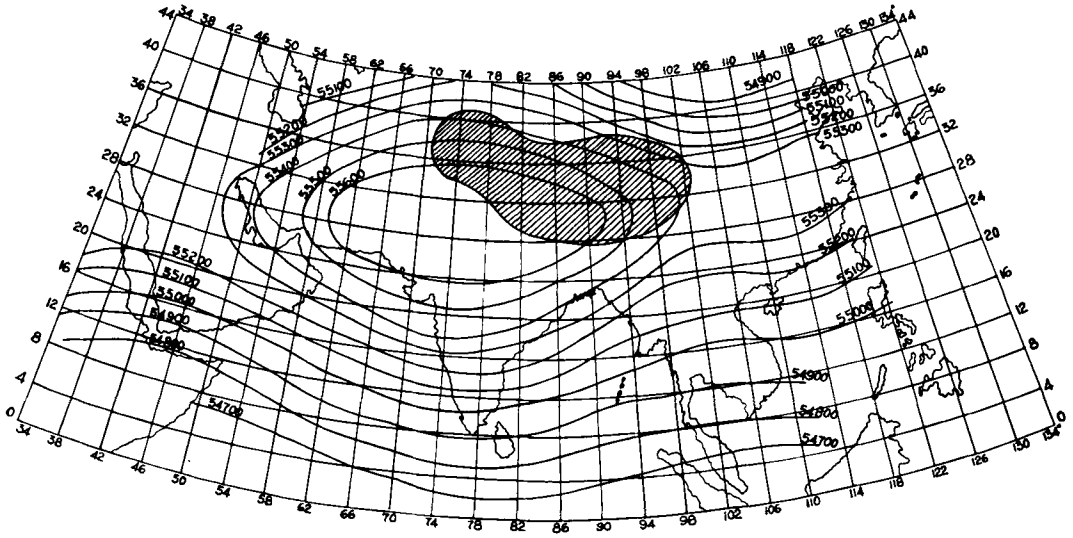

FIG. 4. Mean isobaric contours in feet for July: 100 mb.

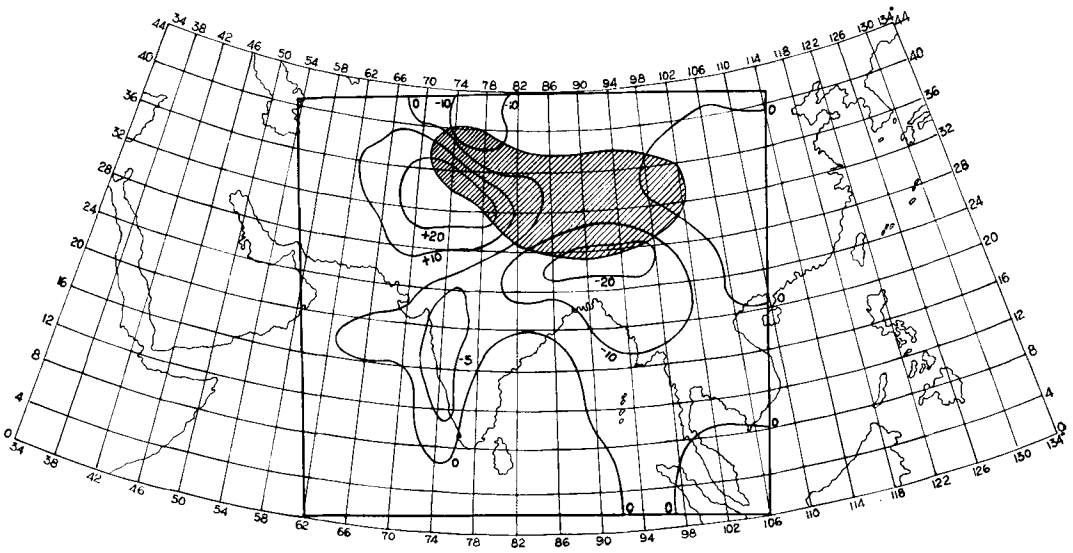

FIG. 5. Mean vertical velocity in cb(12hr)$^{-1}$: 900 mb.

the order of 5–10 kt. A similar value upslope was obtained from the wind data of Gauhati (26.05 N, 91.43 E) on the southeastern edge of the mountains.

4. Variation of ω^* with pressure

In Figs. 5, 6 and 7 we have shown the adiabatically computed ω^* fields at 900, 500 and 200 mb. It may be mentioned in passing that although the adiabatic assumption was used in computing ω^*, none of the other forcing terms, $\mathbf{V}\cdot\nabla\eta$, $\mathbf{V}\cdot\nabla\phi_p$ and gw_0, were neglected. The computations revealed two well marked zones of ω^*, namely, (*a*) an area of marked ascent (negative ω^*) over northeast India and (*b*) a zone of subsidence along the western periphery of the mountains. There were no other regions

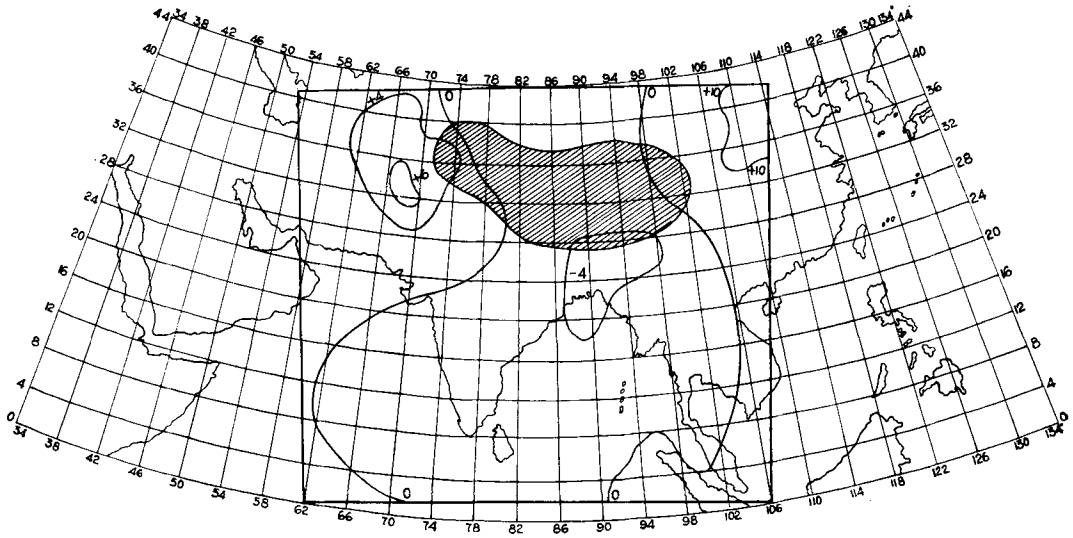

FIG. 6. Mean vertical velocity in cb(12hr)$^{-1}$: 500 mb.

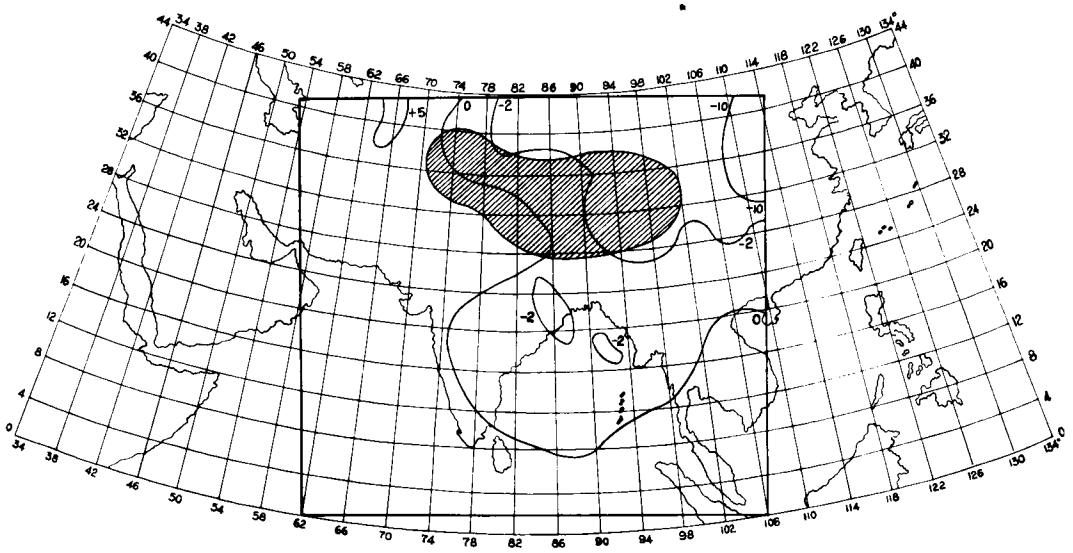

FIG. 7. Mean vertical velocity in cb(12hr)$^{-1}$: 200 mb.

where ω^* was of comparable intensity. Hereafter, we shall refer to the eastern zone of ascent as region A, while the zone of subsidence in northwest India will be designated as region B.

The variation of ω^* with pressure in regions A and B is shown in Fig. 8. We see that ω^* decreases uniformly with pressure in region A, while the variation with pressure in region B is not so well defined. This rather interesting result suggests that the field of ω^* in region A is entirely determined by orographic uplift at the surface.

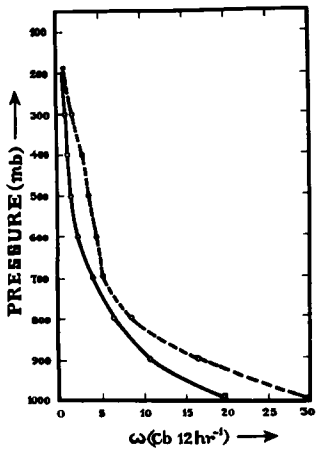

FIG. 8. Variation of vertical velocity with pressure. Full line represents northeast India; dotted line northwest India.

To investigate this aspect of the problem in more detail, let us assume that the field of ω and ϕ_t is determined by the basic equations without $Q, \mathbf{V}\cdot\nabla\eta$, $\mathbf{V}\cdot\nabla\phi_p$ and $L\zeta_0\cdot\mathbf{V}\cdot\nabla H$ is now the only forcing term in the equations. Using primed symbols to denote our new parameters (ω' and ϕ_t') we see that ω' satisfies the equation

$$\nabla^2\omega' + \frac{f^2}{\sigma}\frac{\partial^2\omega'}{\partial p^2} = 0. \tag{4.1}$$

The boundary conditions are

$$(\omega')_1 = 0, \tag{4.2}$$

$$(\omega')_0 = f(x,y), \tag{4.3}$$

where $f(x,y)$ is a function determined by orography. For our present purpose the stability parameter (σ) may be taken to be a simple function of pressure by assuming a constant lapse rate of temperature.

We have $$\frac{f^2}{\sigma} = kp^2, \tag{4.4}$$

where $k = gf^2/RT\,(\gamma_a - \gamma)$, γ_a is the dry adiabatic lapse rate of temperature and T is an average temperature. This form of the stability para-

meter has been used by Soviet meteorologists in recent years (PHILLIPS, BLUMEN and COTE, (1960)).

If we expand $f(x,y)$ in a double Fourier series

$$f(x,y) = \sum_1^\infty \sum_1^\infty A_{m,n} \sin mx \sin ny \qquad (4.5)$$

then the field of ω' satisfying (4.1) and (5.2) is readily shown to be given by the following expression

$$\omega' = \sum_1^\infty \sum_1^\infty A_{m,n} \sin mx \sin ny \left(\frac{p}{p_0}\right)^\varepsilon, \qquad (4.6)$$

where $$2\varepsilon = 1 + \left[1 + 4\left(\frac{m^2+n^2}{k}\right)\right]^{\frac{1}{2}}. \qquad (4.7)$$

The orographically produced vertical velocity (ω'), therefore, decreases with pressure as $(p/p_0)^\varepsilon$.

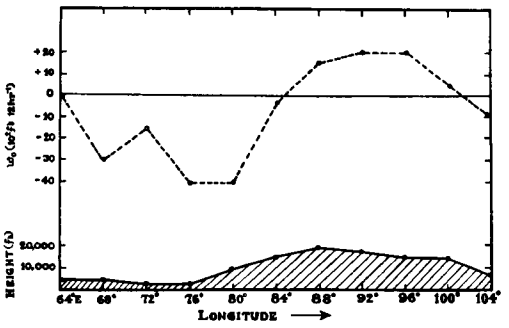

FIG. 9. Meridional variation of w_0 and mountain profile along 30 N.

In Fig. 9 we have shown an east-west section of the mountain profile and the induced vertical velocity (w_0) at the surface along 30 N. But for minor deviations, the similarity between the meridional variation of w_0 and a sinusoidal pattern with a wave length of 1700 km is good. We compared, therefore, the observed variation of ω^* with pressure in region A with the theoretical damping of ω', by setting the wave length to 1700 km and the lapse rate to half the dry adiabatic value. This particular value of the lapse rate was chosen because it was representative of the region under consideration. The comparison, as shown in Fig. 10, revealed a

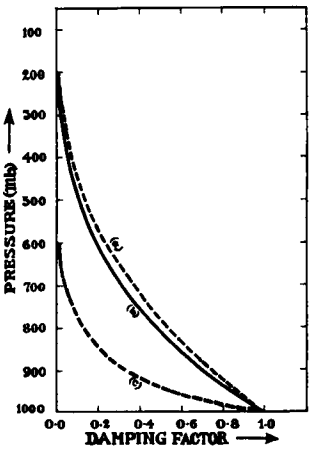

FIG. 10. Computed and observed damping of vertical velocity. (*a*) Observed; (*b*) Computed for wave length 1700 km and $\gamma = 0.5\,\gamma_a$; (*c*) Computed for wave length 500 km and $\gamma = 0.5\,\gamma_a$.

sufficiently close fit to confirm the predominant role of orography. For its theoretical interest, we have also shown the rapid rate of damping for a disturbance of shorter wave length (500 km) in Fig. 10.

5. The computed field of Q

Equation (2.12) gives us the non-adiabatic heat supply which would make the motion steady. An inspection of the fields of ϕ_t^* and ω^* showed that the ω_0^* term in (2.12) was at most ten per cent of the ϕ_{pt}^* term, while the latter was three times larger than the last term. For additional simplicity then, we may replace (2.12) by

$$Q \simeq \frac{p}{k}\phi_{pt}^* = -C_p T_t^*. \qquad (5.1)$$

In other words, a good approximation to Q may be obtained by taking the negative of the adiabatically computed temperature change and multiplying by C_p.

The mean values of ϕ_t^* and the corresponding temperature changes are shown in Table 1 as a function of pressure for both northeast India (A) and the northwestern parts of the country (B). From this table it appears that non-adiabatic sources must be capable of producing an average warming at the rate of 1.6 C(12hr)$^{-1}$ in northeast India, and an average cooling at the rate of 1.2 C(12hr)$^{-1}$ in northwest India.

TABLE 1. *Non-adiabatic heating and resultant temperature change.*

Pressure cb	Mean ϕ_t^* $m^2sec^{-2}(12\,hr)^{-1}$ A	B	Mean pressure, cb	T_t^* $C(12\,hr)^{-1}$ A	B
95	686	−451	90	−3.7	3.7
85	568	−333	80	−2.4	2.7
75	480	−235	70	−1.4	1.4
65	421	−176	60	−1.2	1.2
55	363	−118	50	−1.2	0.5
45	294	−88	40	−0.8	0.8
35	235	−29	30	−0.6	0.3
25	176	0	20	−0.4	0.2
15	118	29	10	−2.4	0.1
5	−568	49	Mean	−1.6	1.2

These sources are most pronounced at the lower levels.

We examined two physical processes which could provide the above requirements for a steady state. They are, (*a*) the latent heat released by precipitation, and (*b*) the cooling produced by outgoing radiation.

The mean precipitation in July over region A and B is 55 cm and 12 cm. A few simple calculations indicate that the latent heat release released by this amount of precipitation could warm the atmosphere by 3 $C(12hr)^{-1}$ in region A, and by 0.6 $C(12hr)^{-1}$ in region B. The predicted non-adiabatic warming is thus of the correct magnitude and sign in northeast India.

To compute the rate of radiative cooling we considered mean upper air soundings from two stations which were representative of region A and B. They are Calcutta (22.0 N, 88.5 E) and New Delhi (28.5 N, 76.5 E). The maximum radiative cooling under clear skies was computed by an Elsasser radiation chart, and the values were 0.5 $C(12hr)^{-1}$ for region A and 0.9 $C(12hr)^{-1}$ for region B.

The maximum cooling by outgoing radiation is thus not sufficient to explain the predicted amount over northwest India. We may, therefore, infer that eddy advection of temperature and vorticity, that is, the non-steady motion which changes from day to day, must provide the additional cooling required over northwest India. Considering the requirement indicated in Table I as our basis, the rate of cooling by this mechanism would appear to be of the order of 1.0 $C(12hr)^{-1}$ in region A and B.

6. Summary and conclusions

It may be desirable to summarize the principal results of this study in the form of the following conclusions:

(1) The geographical orientation of the mountains creates a zone of forced ascent of air over northeast India of the order of 5–10 $cb(12hr)^{-1}$. To counterbalance the area of ascent, there appears to be a well marked zone of subsidence over northwest India. The rate of subsidence is of the same order of magnitude as the rate of ascent.

(2) In northeast India the vertical velocity decreases uniformly with height. The vertical velocity at the surface follows a sinusoidal profile with wave length 1700 km. If we accept this profile on the lower boundary, there is good agreement between the observed and theoretical decrease of ω^* with pressure.

(3) To maintain a steady circulation, non-adiabatic heat sources must be capable of producing warming at the rate of 1.6 $C(12hr)^{-1}$ over northeast India, and cooling at the rate of 1.2 $C(12hr)^{-1}$ over northwest India.

(4) Warming over northeast India could be well explained by the latent heat from heavy precipitation. But estimates of radiative cooling revealed that the predicted cooling over northwest India was too large to be explained by outgoing radiation.

7. Acknowledgements

I am indebted to Professor Norman Phillips for his kind encouragement, and for his pro-

gramme for the ten-layer geostrophic model. I also had the benefit of many helpful discussions with Professor V. P. Starr during the course of this work.

I am also indebted to the Government of India and the International Cooperation Administration, Washington, for leave of absence which enabled me to complete the work at the Massachusetts Institute of Technology, U.S.A.

The computational facilities of IBM 704 were kindly provided by the Computational Research Centre at M.I.T.

REFERENCES

BERKOFSKY, L., and BERTONI, E. A., 1955, Mean topographic charts for the entire hemisphere. *Bull. Am. Meteor. Soc.* **36**, pp. 350–354.

CHARNEY, J. G., 1948, On the scale of atmospheric motions. Geofys. Publn. **17**, 17 pp.

CHARNEY, J. G., and PHILLIPS, N. A., 1953, Numerical integration of the quasi-geostrophic equations for barotropic and simple baroclinic flow. J. Meteor. **10**, pp. 71–99.

PHILLIPS, N. A., BLUMEN, W., and COTE, O., 1960, *Numerical Weather Prediction in the Soviet Union.* Cambridge, Massachusetts Institute of Technology, 61 pp.